

X-ray Analysis of Fe doped ZnO Nanoparticles by Williamson-Hall and Size-Strain Plot

Y. T. Prabhu, K. Venkateswara Rao, V. Sesha Sai Kumar, B. Siva Kumari

Abstract—In the preparation of Fe doped ZnO a novel process is used with different doping concentrations from 2% to 10% by surfactant assisted combustion synthesis. The synthesized samples were characterized with X-ray diffraction particle analyzer and TEM. From X-ray diffraction, it was observed Fe-doped ZnO nanoparticles (NPs) have hexagonal wurtzite structure and further crystallite sizes were decreased with increasing doping concentrations. Transmission electron microscopy (TEM) showed that powder was polycrystalline in nature with random distribution of nano grained Fe doped ZnO. Using X-ray broadening crystalline development in the Fe doped ZnO-NPs was investigated. The crystallite sizes and lattice strain on the peak broadening of Fe doped ZnO-NPs were studied using Williamson-Hall (W-H) analysis and size-strain plot. Strain, stress and energy density parameters were calculated for the XRD peaks of all the samples using (UDM), uniform stress deformation model (USDM), uniform deformation energy density model (UDEDM) and by the size-strain plot method (SSP). The results of mean particle size of Fe doped ZnO-NPs showed an inter correlation with W-H analysis, SSP, and TEM results.

Key words: Fe Doped ZnO, Surfactant Assisted Combustion Synthesis, XRD, TEM.

I. INTRODUCTION

The important semiconductor which has been studied very extensively is Zinc Oxide (ZnO) for its primary and industrial importance. ZnO has typical properties such as transparency in the visible range, direct band gap, high electrochemical stability, toxic absorbance and plenty in nature. [1] The III–V and II–VI based dilute magnetic semiconductors (DMS) are very encouraging materials for spintronics applications as DMS show ferromagnetic nature at room temperature.[2] Extensive studies were made on transition metal (TM) doped II–VI and III–V compound semiconductors (such as Fe, Co, Ni, Mn etc.).[3-4] Deviations from perfect crystallinity extends infinitely in all directions, leads to broadening of the diffraction peaks. The crystallite size and lattice strain are the two main properties which could be extracted from the peak width analysis. Due to the formation of polycrystalline aggregates [5] the crystallite size of the particle is not the same as the particle size. The crystal imperfections could be measured from the distributions of lattice constants.

The basis of strain also includes contact or sinter stress, grain boundary triple junction stacking faults and coherency stress [6]. In different ways Bragg peak are affected by crystallite size and lattice strain which increase the peak width and intensity shifting the 2θ peak position accordingly. The crystallite size varies as $1/\cos \theta$ and stain varies as $\tan \theta$ from the peak width. The size and strain effects on peak broadening are known from the above difference of 2θ . W-H analysis is an integral breadth method. Size-induced and strain-induced broadening are deintricated by considering the peak width as a function of 2θ [7]. In this paper firstly the novel surfactant assisted combustion synthesis method was used to prepare Fe-doped ZnO nanoparticles secondly comparative study of the mean particle size of Fe-doped ZnO nanoparticles from tem measurements and from the powdered XRD. Using Williamson- Hall modified form strain, uniform deformation model (UDM), uniform stress deformation model (USDM), uniform deformation energy-density model (UDEDM) and the size-strain plot method (SSP) provided information on the stress-strain relation and the strain ϵ as a function of energy density (u) were estimated.

II. EXPERIMENTAL DETAILS

A. Sample synthesis and geometric characterization review Stage

The surfactant assisted combustion synthesis method paved the way to reduce the size of the particle with cost and time efficient. As many properties are dependent on the size and morphology this method helped to achieve the desired results. $Zn(NO_3)_2$ and $Fe(NO_3)_3$ oxidizers are taken in required stoichiometric amounts in water. After that 0.15 M of Glycine fuel was added to the clear solution formed by oxidizers, then the solution was added with 0.025 M of non-ionic surfactant Triton-X 100. The mixture of solution was then kept on a hot plate. As the temperature increased to $100^\circ C$ water slowly evaporated which led to increase in the viscosity of liquid and finally smoldering started leading to self-ignition forming the final product. The final product obtained was then calcined at $200^\circ C$ for 1 hr to get the pure Fe-doped ZnO nanoparticles. Using X-ray diffractometry Phase growths of the ZnO-NPs were studied. The complete procedure can be found in the literature [8].

III. RESULTS AND DISCUSSION

A. XRD analysis

Fe-doped ZnO and ZnO nanoparticles are characterized using XRD. In Fig 1 it can be observed that the diffraction peaks exhibit a single phase wurtzite structure (space group $p63mc$, JCPDF #36-1451) and exclude the existence of secondary or impure phases.

Manuscript published on 30 April 2013.

* Correspondence Author (s)

Y. T. Prabhu*, Centre for Nano Science and Technology, IST, JNTU Hyderabad, AP, India.

Dr. K. Venkateswara Rao, Centre for Nano Science and Technology, IST, JNTU Hyderabad, AP, India

Dr. B. Siva Kumari, Botany Department, Andhra Loyola College, Vijayawada, AP, India

V. Sesha Sai Kumar, Centre for Nano Science and Technology, IST, JNTU Hyderabad, AP, India.

© The Authors. Published by Blue Eyes Intelligence Engineering and Sciences Publication (BEIESP). This is an [open access](http://creativecommons.org/licenses/by-nc-nd/4.0/) article under the CC-BY-NC-ND license <http://creativecommons.org/licenses/by-nc-nd/4.0/>.

It is clearly inferred that Fe ions successfully exist in the lattice sites rather than interstitial sites. The peak position at $2\theta = 34.44^\circ$ which corresponds to (002) plane of ZnO has hexagonal wurtzite structure [9].

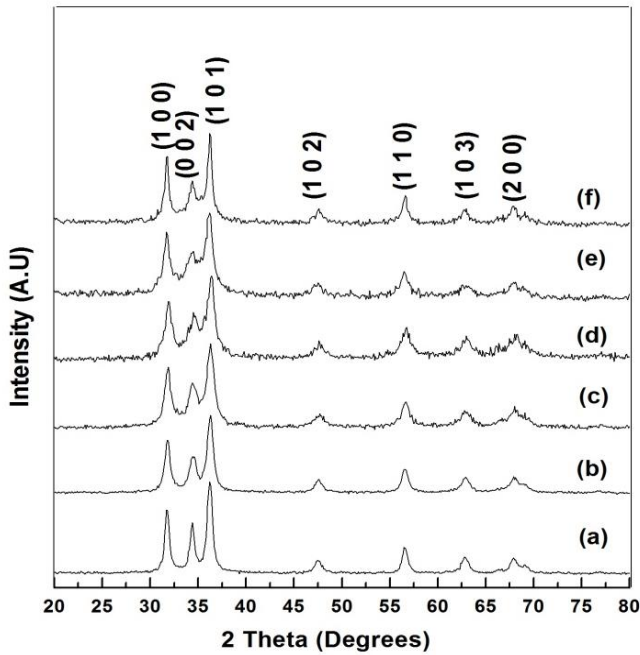


Fig. 1. XRD patterns of Fe-doped ZnO nanoparticles. (a) undoped (b) 2% of Fe; (c) 4% of Fe; (d) 6% of Fe; (e) 8% of Fe; and (f) 10% of Fe.

As the concentration of Fe changes the peak (002) changes predominantly the peak (002) of all the samples are drawn in Fig 1(a). The peak (002) shifted towards higher angle compared with the undoped ZnO and there was decrease in intensity with increase in Fe concentration. This shifting in peak position and decrease in intensity reflect that Fe is successfully replaced Zn in ZnO matrix as diffraction of X-ray changes. It also suggests that with the increase in Fe concentration the crystalline quality of ZnO declines gradually [10].

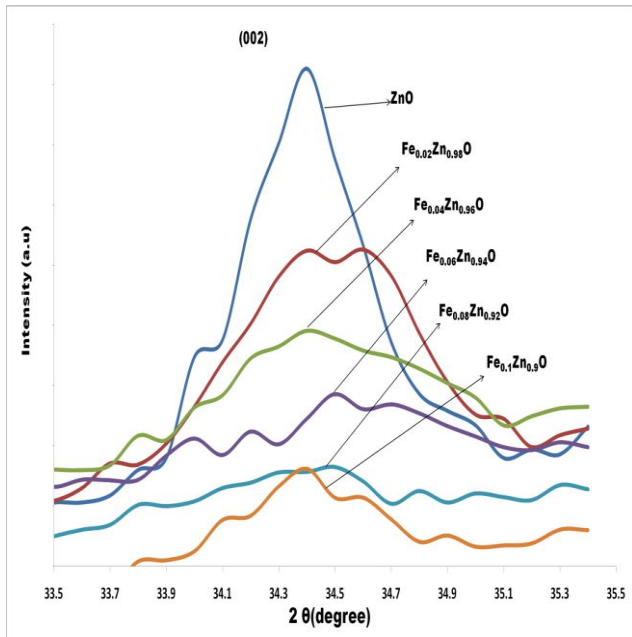


Fig 1(a). XRD data of the (002) peak for undoped and Fe-doped ZnO nanoparticles.

One, ZnO crystal lattice can restrain crystallization due to Fe doping. The other reason can be ascribed to smaller crystallite size of $Fe_xZn_{1-x}O$. The lattice constants of $Fe_xZn_{1-x}O$ and ZnO are given in the Table. 1

Table. 1. Unit cell Parameters of Undoped and Fe-doped ZnO nanoparticles.

x (Fe addition)	Unit Cell parameters		Cell Volume (\AA^3)	Scherrer Size	c/a ratio
	a	c			
0	3.252	5.214	47.76	24.3	1.602
0.02	3.249	5.214	47.88	17.3	1.600
0.04	3.2536	5.216	47.92	13.5	1.603
0.06	3.256	5.220	47.93	12.3	1.600
0.08	3.254	5.213	47.81	10.2	1.597
0.1	3.248	5.207	47.58	9	1.602

$$\frac{1}{d^2} = \frac{4}{3} \left(\frac{h^2 + hk + k^2}{a^2} \right) + \frac{l^2}{c^2} \quad (1)$$

$$v = \frac{\sqrt{3}}{2} a^2 c = 0.866 a^2 c \quad (2)$$

B. Scherrer method

Crystallite size and lattice strain due to dislocation can be calculated from peak broadening using XRD [11]. X-ray line broadening method was used to determine the particle size of the Fe doped ZnO nanoparticles using Scherrer equation. $D = (k\lambda/\beta_D \cos\theta)$, where D is the particle size in nanometers, λ is the wavelength of the radiation (1.54056 \AA for $CuK\alpha$ radiation), k is a constant equal to 0.94, β_D is the peak width at half-maximum intensity and θ is the peak position. Both instrument- and sample dependent effects are combination of the Bragg peak breadth. To remove these aberrations, it is needed to assemble a diffraction pattern from the line broadening of a standard material such as silicon to determine the instrumental broadening. The instrument-corrected broadening [12] β_D corresponding to the diffraction peak of Fe doped ZnO was estimated using the relation:

$$\beta^2_D = [\beta^2_{measures} - \beta^2_{instrumental}] \quad (3)$$

$$D = \frac{k\lambda}{\beta_D \cos\theta} \Rightarrow \cos\theta \frac{k\lambda}{D} \left(\frac{1}{\beta_D} \right) \quad (4)$$

C. Williamson-Hall methods

Crystal imperfections and distortion of strain-induced peak broadening are related by $\epsilon \approx \beta_s/\tan\theta$. There is an extraordinary property of Eq. (4) which has the dependency on the diffraction angle θ . Scherrer-equation follows a $1/\cos\theta$ dependency but not $\tan\theta$ as W-H method. This basic difference was that both microstructural causes small crystallite size and microstrain occur together from the reflection broadening.

Depending on different θ positions the separation of size and strain broadening analysis is done using Williamson and Hall. The following results are the addition of the Scherrer equation and $\epsilon \approx \beta_s/\tan\theta$.

$$\beta_{hkl} = \beta_s + \beta_D \tag{5}$$

$$\beta_{hkl} = \left(\frac{k\lambda}{D \cos\theta}\right) + 4\epsilon \tan\theta \tag{6}$$

Rearranging Eq. (6) gives:

$$\beta_{hkl} = \left(\frac{k\lambda}{D}\right) + 4\epsilon \sin\theta \tag{7}$$

Here Eq. (7) stands for UDM where it is assumed that stain is uniform in all crystallographic directions. $\beta\cos\theta$ was plotted with respect to $4\sin\theta$ for the peaks of Fe doped ZnO. Strain and particle size are calculated from the slope and y-intercept of the fitted line respectively. From the lattice parameters calculations it was observed that this strain might be due to the lattice shrinkage. The UDM analysis results are shown in Fig 2.

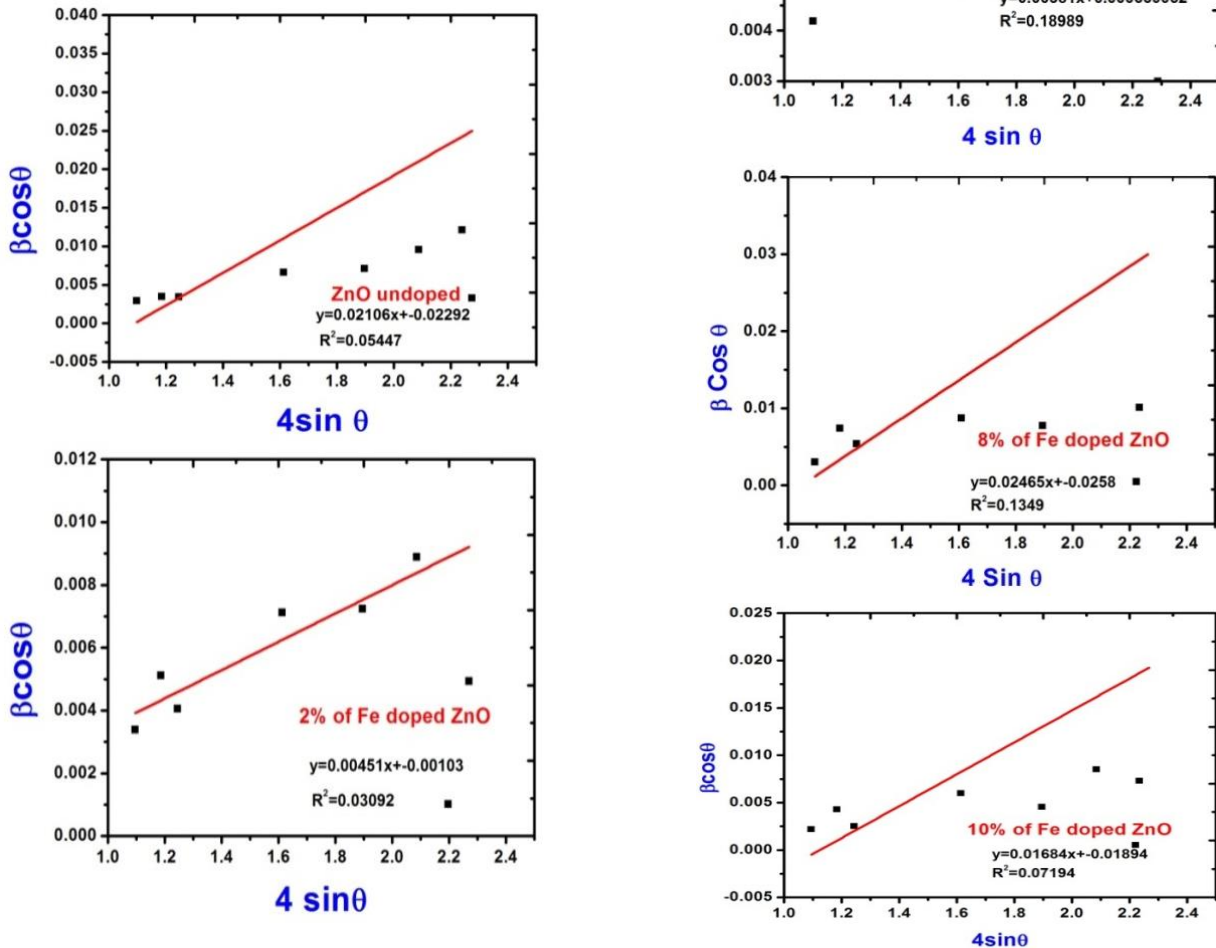


Fig. 2. The W-H analysis of Fe-doped ZnO nanoparticles. Undoped, 2% of Fe, 4% of Fe, 6% of Fe, 8% of Fe, and 10% of Fe assuming UDM. Fit to the data, the strain is extracted from the slope and the crystalline size is extracted from the y-intercept of the fit.



From Uniform Stress Deformation Model (USDM) strain is calculated from the Hook's Law maintaining linea proportionality between stress and strain by $\sigma=Y\varepsilon$, where σ is the stress and Y is the Young's modulus. This Hook's law is valid for a significantly small strain. Supposing a small strain to be present in the Fe doped ZnO, Hooke's law can be used here. Applying the Hooke's law approximation to Eq. (7) yields:

$$\beta_{hkl} \cos \theta = \left(\frac{k\lambda}{D}\right) + \left(\frac{4\sigma \sin \theta}{Y_{hkl}}\right) \quad (8)$$

For a hexagonal crystal, Young's modulus is given by the following relation [13]:

$$Y_{hkl} = \left(\frac{[h^2 + \frac{(h+2k)^2}{3} + \frac{(al)^2}{c}]^2}{S_{11}(h^2 + \frac{(h+2k)^2}{3})^2 + S_{33}(\frac{al}{c})^4 + (2S_{13} + S_{44})(h^2 + \frac{(h+2k)^2}{3})\frac{(al)^2}{c}} \right) \quad (9)$$

where s_{11} , s_{13} , s_{33} , s_{44} are the elastic compliances of ZnO with values of 7.858×10^{-12} , -2.206×10^{-12} , 6.940×10^{-12} , $23.57 \times 10^{-12} \text{ m}^2 \text{ N}^{-1}$, respectively [14]. Young's modulus, Y , for hexagonal Fe doped ZnO was calculated as $\approx 130 \text{ GPa}$. $4\sin\theta/Y_{hkl}$ and $\beta\cos\theta$ were taken on x- axis and y-axis respectively. The USDM plots for Fe doped ZnO are shown in the Fig. 3. The stress is calculated from the slope.

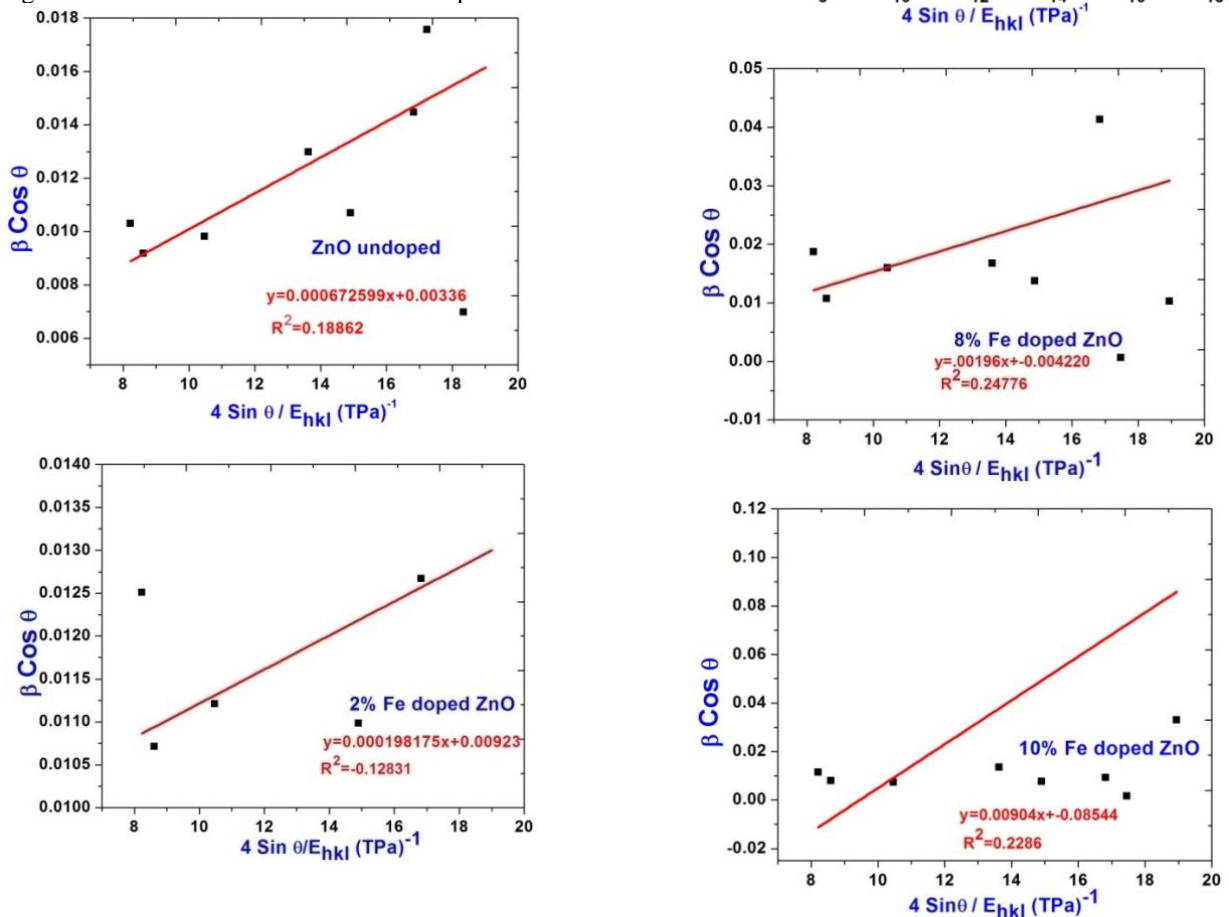


Fig. 3. The modified form of W-H analysis assuming USDM for Fe-doped ZnO nanoparticles. Undoped, 2% of Fe, 4% of Fe, 6% of Fe, 8% of Fe and 10%. Fit to the data, the stress is extracted from the slope and the crystalline size is extracted from the y-intercept of the fit.



The energy density of a crystal was calculated from a model called Uniform Deformation Energy Density Model (UDEM). From Eq.8 we need to implicit that crystals are to be homogeneous and isotropic nature. The energy density u can be calculated from $u = (\epsilon^2 Y_{hkl})/2$ using Hooke's law. The Eq. 8 can be modified according the energy and strain relation.

$$\beta_{hkl} = \left(\frac{k\lambda}{D}\right) + (4 \sin \theta \left(\frac{2u}{Y_{hkl}}\right)^{1/2}) \quad (10)$$

$4 \sin \theta (2u/Y_{hkl})^{1/2}$ and $\beta_{hkl} \cos \theta$ were taken on x-axis and y-axis respectively. From the slope the anisotropic energy density u was calculated and the crystallite size D from the Y-intercept from Fig 4. We know that $\sigma = \epsilon Y$ and $u = (\epsilon^2 Y_{hkl})/2$ the stress σ was calculated as $u = (\epsilon^2 Y_{hkl})/2$.

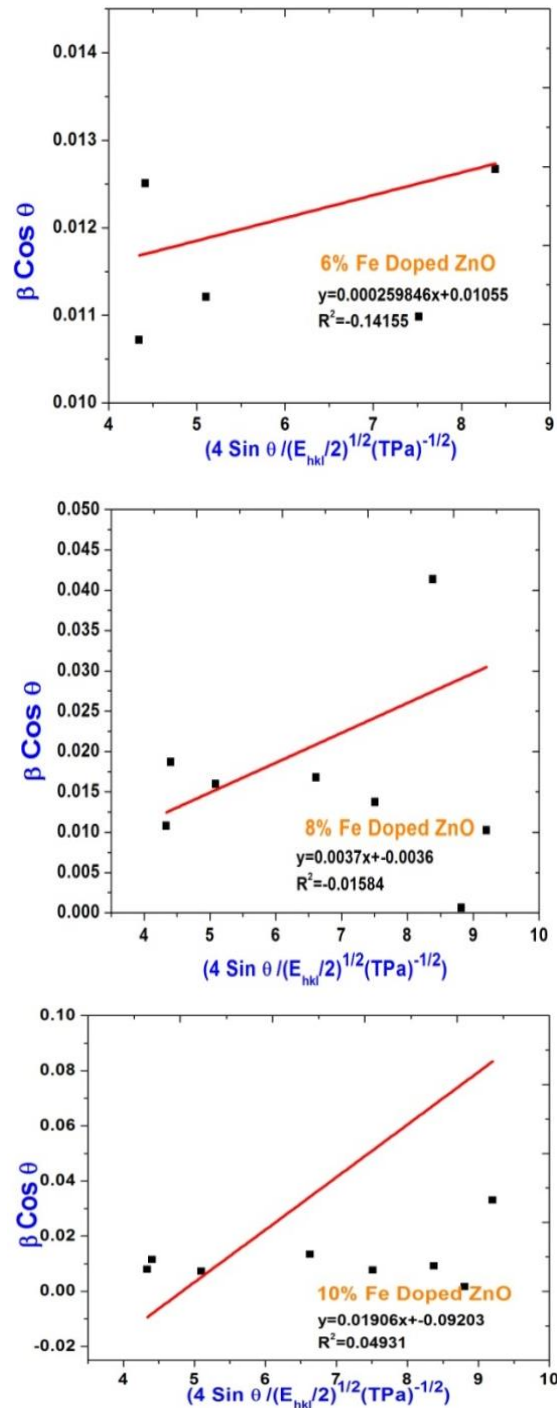
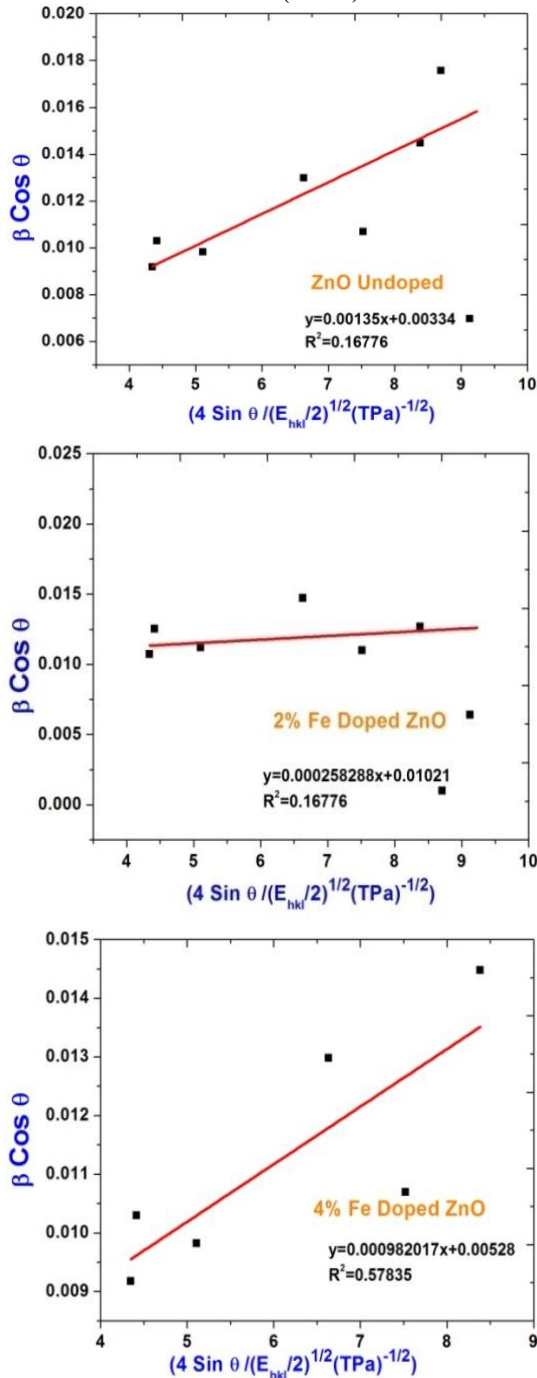


Fig. 4. The modified form of W-H analysis assuming UDEM for Fe-doped ZnO nanoparticles. Undoped, 2% of Fe, 4% of Fe, 6% of Fe, 8% of Fe and 10% of Fe. Fit to the data, the density of energy is extracted from the slope and the crystallite size is extracted from the y-intercept of the fit.

D. Size-strain plot method

Williamson-Hall plot has illustrated that line broadening was basically isotropic. Due to microstrain contribution the diffracting domains were isotropic. Size-strain parameters can be obtained from the “size-strain plot” (SSP). This has a benefit that less importance is given to data from reflections at high angles. In this estimation, it is assumed that profile is illustrated by “strain profile” by a Gaussian function and the “crystallite size” by Lorentzian function [15]. Hence we have



$$(d_{hkl}\beta_{hkl} \cos\theta)^2 = \frac{k}{D} (d^2_{hkl}\beta_{hkl} \cos\theta) + \left(\frac{\varepsilon}{2}\right)^2 \quad (12)$$

where K is a constant, shape of the particles for spherical particles it is given as 3/4. In Fig. 5, $d^2_{hkl}\beta_{hkl} \cos\theta$ and $(d_{hkl}\beta_{hkl} \cos\theta)^2$ were taken on x-axis and y-axis respectively for all peaks of Fe doped ZnO-NPs with the wurtzite hexagonal phase from $2\theta=20^\circ$ to $2\theta=80^\circ$. The particle size is calculated from the slope linearly fitted data and the root of the y-intercept gives the strain.

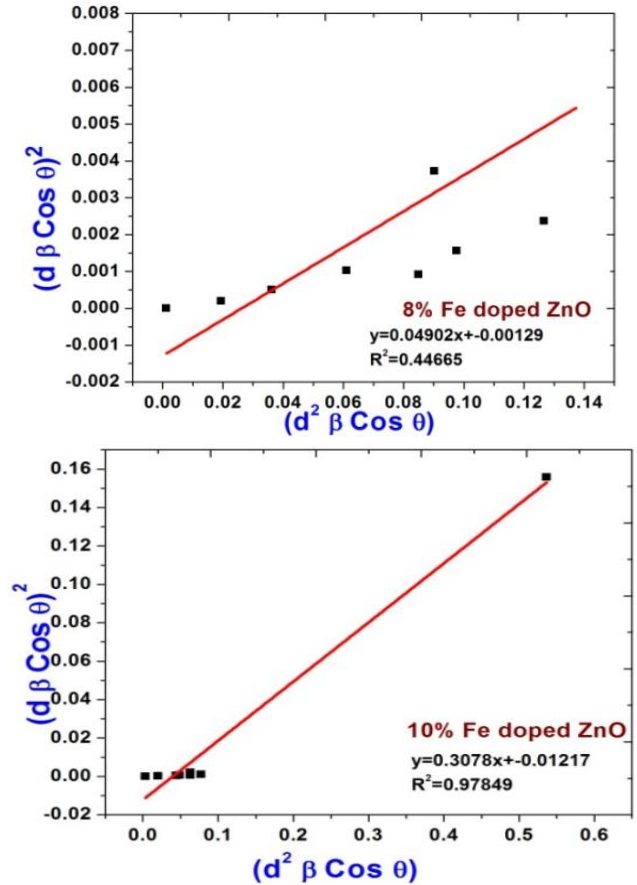
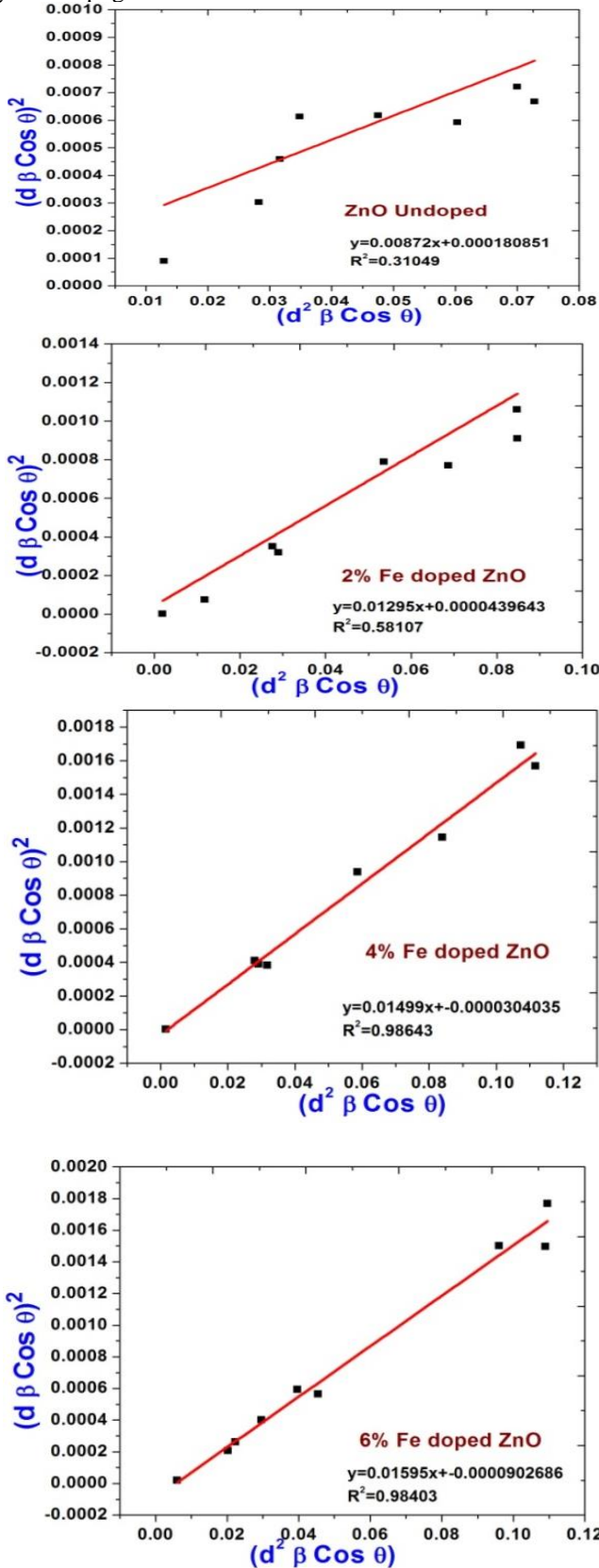


Fig. 5. The SSP plot of Fe-doped ZnO nanoparticles. Undoped; 2% of Fe; 4% of Fe; 6% of Fe; 8% of Fe; and 10% of Fe. The particle size is achieved from the slope of the linear fitted data and the root of y-intercept gives the strain.

E. TEM method

The size and shape of the NPs could be best examined by TEM micrographs. Fig. 6 displays a TEM image of undoped and Fe doped ZnO-NPs. It was observed that the morphology of the ZnO-NPs was spherical and with a smooth surface. Fig. 7 displays SAED pattern of Fe doped ZnO nanoparticles. In the table 2, the results attained from Scherrer method, UDM, USDM, UDEDM, SSP models and TEM are summarized. The average crystallite size of the Fe doped ZnO NPs decreased with increase in the Fe concentration from the different models implying that the inclusion of strain in different forms has very little effect on the average crystallite size.

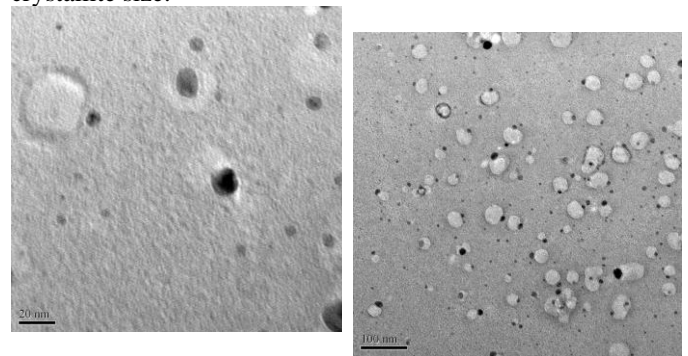


Fig. 6. TEM micrographs of Undoped and Fe-doped ZnO nanoparticles. This figure shows a nonuniform strain for some of the ZnO-NPs.



Table. 2. Geometric parameters of Undoped and Fe-doped ZnO nanoparticles.

Sample Name	Williamson-Hall Method									Size-Strain Plot Method	
	UDM		USDM			UEDM					
% of Fe	D (nm)	ϵ no Unit $\times 10^{-3}$	D (nm)	ϵ no Unit $\times 10^{-3}$	σ (Mpa)	D (nm)	ϵ no Unit $\times 10^{-3}$	σ (Mpa)	u (kJm^{-3})	D (nm)	ϵ no Unit $\times 10^{-3}$
0	22.5	1.38	22.98	1.45	110.32	22.2	1.38	108.32	44.57	20.3	1.42
0.02	15.3	2.031	15.76	2.12	116.54	15.4	2.25	115.23	49.24	14.5	2.19
0.04	11.4	2.86	11.91	2.75	119.25	11.2	2.66	118.85	54.67	11.02	2.8
0.06	10.7	3.5425	10.88	3.62	121.32	10.1	3.37	121.54	62.63	9.9	3.53
0.08	8.1	4.2135	8.79	4.51	123.14	8.41	4.18	124.57	74.51	8.1	4.38
0.1	7.5	5.5314	7.93	5.35	124.85	7.31	5.24	126.21	87.54	7.2	5.29

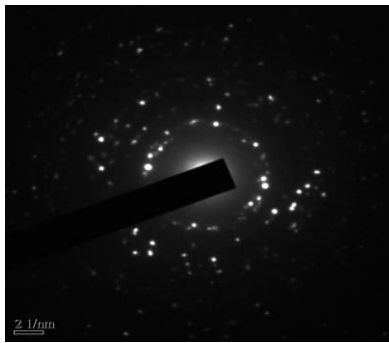


Fig.7. SAED pattern of Fe doped ZnO

IV. CONCLUSIONS

The novel surfactant assisted combustion synthesis method was useful in successfully doping Fe in ZnO nanoparticles and as a function of doping concentrations and characterized by powder XRD and TEM. The XRD pointed out that the wurtzite structure Fe doped ZnO Nano particles were free from any pyrochlore phase even after doping with Fe as Fe was slightly doped. It is clearly observed that the peak (002) position shifted towards bigger angle compared to the undoped ZnO and also it was seen that the peaks decreased in intensity with increase in Fe concentration. This shifting in peak position and decrease in intensity reflected that Fe was successfully replaced Zn in ZnO matrix as diffraction of X-ray changes. This broadening was analyzed by the Scherrer formula, modified forms of W-H analysis and the size-strain plot method. From the results, it was observed that the strain value decreased but the particle size increased as doping concentration increased. The TEM results were in good agreement with the results of the W-H and the SSP methods.

REFERENCES

- [1] V. R. Shinde, T. P. Gujar, C. D. Lokhande, R. S. Mane, and S. H. Han, "Mn doped and undoped ZnO films: A comparative structural, optical and electrical properties study" *Mater. Chem. Phys.* Vol 96, 2006, pp 326-330.
- [2] S. Y. Yang, A. B. Pakhomov, S. T. Hund, and C. Y. Wong, "Room temperature magnetism in sputtered (Zn,Co)O films" *IEEE Trans. Magn.* Vol 38, 2002, pp 2877 – 2879.
- [3] C. J. Cong, J. H. Hong, Q. Y. Liu, L. Liao, and K. L. Zhang, "Synthesis, structure and ferromagnetic properties of Ni-doped ZnO nanoparticles" *Solid State Commun.* Vol.138, 2006, pp 511-515.
- [4] T. Dietl, H. Ohno, F. Matsukura, J. Cibert, and D. Ferrand, *Science* Vol 287, 2000, pp 1019.
- [5] K. Ramakanth, Basic of Diffraction and Its Application. I.K. International Publishing House Pvt. Ltd, New Dehli, 2007.

- [6] Jian-Min Zhang, Yan Zhang, Ke-Wei Xu, Vincent Ji, "General compliance transformation relation and applications for anisotropic hexagonal metals" *Solid State Commun.* Vol 139, 2006 pp 87- 91.
- [7] C. Suranarayana, M.G. Norton, X-ray Diffraction: A Practical Approach New York 1998.
- [8] A. Khorsand Zak, M. Ebrahimzadeh Abrishami, W.H. Abd. Majid, Ramin Yousefi, S.M. Hosseini", *Ceram. Inter.* Vol. 37, pp 393-398, 2011.
- [9] N. Padmavathy and R. Vijayaraghavan, "Enhanced bioactivity of ZnO nanoparticles—an antimicrobial study" *Sci. Technol. Adv. Mater.* 9, 2008. doi:10.1088/1468-6996/9/3/035004
- [10] Linhua Xu, Xiangyin Li, "Influence of Fe-doping on the structural and optical properties of ZnO thin films prepared by sol-gel method" *J. Cryst. Growth*, Vol. 312, 2010, pp 851-855.
- [11] R. Yogamalar, R. Srinivasan, A. Vinu, K. Ariga, A.C. Bose, "X-ray peak broadening analysis in ZnO nanoparticles" *Solid State Commun.* Vol. 149 2009, pp. 1919-1923.
- [12] K.D. Rogers, P. Daniels, "An X-ray diffraction study of the effects of heat treatment on bone mineral microstructure" *Biomaterials*, Vol.23, 2002, pp 2577-2585
- [13] Jian-Min Zhang, Yan Zhang, Ke-Wei Xu, Vincent Ji, "General compliance transformation relation and applications for anisotropic hexagonal metals" *Solid State Commun.* Vol.139, 2006, pp 87-.
- [14] J.F. Nye, Physical Properties of Crystals: Their Representation by Tensors and Matrices. Oxford, New York, 1985.
- [15] M.A. Tagliente, M.Massarò, "Strain-driven (0 0 2) preferred orientation of ZnO nanoparticles in ion-implanted silica" *Nucl. Instrum Methods Phys. Res. B.* Vol. 266, 2008, pp.1055 -1061.



Y. T. Prabhu is a student who completed M.Sc from centre for Nanoscience and Technology (CNST), Institute of Science and Technology, Jawaharlal Nehru Technological University Hyderabad. He has published his works in American Scientific Publishers in the journal Advanced Science, Engineering and Medicine; Scientific Research in the journal Advances in Nano Particle. He has published a book titled "Novel Synthesis of Fe doped Zinc Oxide Nano particles and Properties" with ISBN 978-3-659-35372-7. His present research focus is on CNT's.



Dr. K. Venkateswara Rao is working as Associate Professor of Nanotechnology in Centre for Nanoscience and Technology (CNST), Institute of Science and Technology, Jawaharlal Nehru Technological University Hyderabad. He received M.Sc degree in Physics from University of Hyderabad and M.Tech degree in computer science and engineering from JNT University Hyderabad. He has published many books in the field of Nano Technology and published many papers in reputable journals. His present research is focus on: "Nano-Magnetic materials synthesis and characterization thin films".



X-ray Analysis of Fe doped ZnO Nanoparticles by Williamson-Hall and Size-Strain Plot Methods



V. Sessa Sai Kumar is working as Lecturer in Centre for Nanoscience and Technology (CNST), Institute of Science and Technology, Jawaharlal Nehru Technological University Hyderabad. He received M.Tech, Nanotechnology from JNT University Hyderabad. He has published a book in the field of Nano Technology with ISBN 978-3-659-34512-8 and published many papers in journals. He is pursuing Ph.D in

Nano Science and Technology.



Dr. B. Siva Kumari is an Associate Professor in Botany Andhra Loyola College, Vijayawada. She pursued her Ph.D from Choudary Charan Singh University, India. She guides research scholars in the fields of Botany and Nano-Biotechnology. She has published many books in the field of Botany and Nano Biotechnology. She has published many papers in reputable journals. Her hobby is to Survey and to identify flora and conducting environmental awareness programmes.